Prediction and Experimental Characterization of the Molecular Architecture of FRP and ATRP Synthesized Polyacrylate Networks

Miguel A. D. Gonçalves,[1] *Rolando C. S. Dias,**[1] *Mário Rui P. F. N. Costa*[2]

Summary: This work reports experimental and modeling studies concerning the conventional (FRP) and atom transfer radical polymerization (ATRP) of acrylate/diacrylate monomers. In the framework of a recently developed general approach, kinetic models including crosslinking reactions and branching by chain transfer to polymer are discussed for FRP and ATRP polymerization systems. Besides molecular weight distribution (MWD), fairly good predictions of the *z*-average radius of gyration could be obtained for these non-linear polymers. A set of experiments was performed at 1 L scale in a batch reactor using *n*-butyl acrylate (BA) or methyl acrylate (MA) as monovinyl monomers and 1,6-Hexanediol diacrylate (HDDA) or bisphenol A ethoxylate diacrylate (BEDA) as crosslinkers. In FRP experiments, AIBN was used as initiator and ATRP polymerizations were initiated by ethyl 2-bromopropionate (EBrP) and mediated by CuBr using PMDETA (*N,N,N′,N″,N″*-pentamethyldiethylenetriamine) as ligant. Polymerizations were carried out in solution at 60 °C with different dilutions using toluene and DMF as solvents. Products formed at different polymerization times were analyzed by SEC/RI/MALLS yielding average MW, MWD, *z*-average radius of gyration and monomer conversion. Important differences in the molecular architecture of the synthesized FRP and ATRP highly branched polyacrylates have been identified. Comparisons of experimental results with predictions have put into evidence the important effect of intramolecular cyclizations at all dilutions, even with ATRP polymerizations.

Keywords: ATRP; branching; crosslinking; modeling; radius of gyration

Introduction

Non-linear radical polymerizations are used to produce soluble and insoluble crosslinked materials with important applications in several domains, such as biomedicine, pharmaceutics, biotechnology, environment and microelectronics. Conventional free radical polymerization (FRP) leads to microgels (very high molecular weight soluble non-linear polymers) and gels (insoluble materials) with inhomogeneous structures due to the combination of slow initiation, fast propagation and termination.[1] Controlled radical polymerization (CRP) has been recently exploited to increase the homogeneity of these kinds of products.[2–4]

Nowadays, there are some important open issues in this field, namely concerning the impact of intramolecular cyclizations/unequal functional group reactivity in the structure of these materials. The design of new operation conditions to manipulate the molecular architecture (e.g. operation in semi-batch reactor[5]) or the control of gelation and/or post gel properties are

[1] LSRE-Instituto Politécnico de Bragança, Quinta de Santa Apolónia, 5300 Bragança, Portugal
Fax: (+351)273313051;
E-mail: rdias@ipb.pt
[2] LSRE-Faculdade de Engenharia da Universidade do Porto, Rua Roberto Frias s/n, 4200-465 Porto, Portugal
Fax: (+351)225081666
E-mail: mrcosta@fe.up.pt

other important aspects concerning the polymer reaction engineering of these kinds of polymerization systems.

This work reports experimental and theoretical studies concerning the FRP and ATRP production of acrylate/diacrylate microgels. Some important features of the molecular architecture of these materials are investigated and differences between the two kinds of polymerization systems are studied. The impact of the synthesis conditions on the structure of the products is assessed in order to develop tools for the design of materials with improved end use properties.

Experimental

Experiments were carried out using a 2 L reactor of which a detailed description has already been presented elsewhere.[5] In ATRP experiments, *N,N*-dimethylformamide (DMF) of 99.8% purity, ethyl 2-bromopropionate (EBrP) of 99% purity, Cu(I)Br of 98% purity, *N,N,N′,N″,N″*-pentamethyldiethylenetriamine (PMDETA) of 99% purity, *n*-butyl acrylate (BA) of 99% purity stabilized with 10 to 55 ppm monomethyl ether hydroquinone (MEHQ), methyl acrylate (MA) of 99% purity stabilized with 100 ppm MEHQ, 1,6-Hexanediol diacrylate (HDDA) of 80% purity stabilized with 100 ppm MEHQ, bisphenol A ethoxylate diacrylate (BEDA) with $\overline{M}_n \simeq 688$ of 99% purity stabilized with 250 ppm MEHQ were purchased from Sigma Aldrich and used as received. In FRP experiments the same monomers and crosslinkers were used and AIBN of 98% purity and toluene of 99.7% purity were also purchased from Sigma Aldrich and used as received. Monomers were used as received to mimic the industrial practice, and the presence of inhibition/retardation of polymerization is taken into account in kinetic modeling.

In ATRP experiments (see Table 1), DMF, acrylate monomer, diacrylate monomer, PMDETA and CuBr were premixed at 60 °C for at least 30 min in a volumetric flask. Good solubility of CuBr in the polymerization system was observed. That mixture was afterwards charged to the reactor, which had previously been purged with argon at a flow rate of 40 cm^3/min, and brought up to the polymerization temperature (60 °C). When the temperature set-point was attained, the bubbling process was maintained for one hour before initiation (as well as for the whole polymerization). Then, the initiator (EBrP) was added to the system defining $t = 0$. At prescribed polymerization times, samples of polymer were withdrawn from the reactor and analyzed by SEC/RI/MALLS. Similar procedures were performed in FRP experiments (see Table 2) with exception of the pre-mixing period which is absent.

Molecular weights and average molecular radius of gyration in THF were measured with a Polymer Laboratories PL-GPC-50 integrated SEC system with a differential refractometer working at 950 ± 30 nm attached to a Wyatt Technology DAWN8$^+$ HELEOS 658 nm Multi Angle Laser Light Scattering (MALLS) detector. The polymer samples were fractioned by molecular size using a train of 3 GPC columns PL gel (300 × 7.5 mm) with nominal particle size 10 μm and pore type MIXED-B-LS, maintained at constant

Table 1.
Description of a set of experiments performed in the study of the ATRP copolymerization of Acrylate/Diacrylate monomers at 60 °C.

Run	M	[M]	CL	y_C (%)	M/EBrP/CuBr/PMDETA	V_M (%)
1	MA	2.44	–	0.0	50/1/0.45/0.5	22
2	BA	2.44	–	0.0	50/1/0.45/0.5	35
3	BA	2.41	HDDA	2.0	50/1/0.45/0.5	35
4	BA	2.28	HDDA	10.0	50/1/0.45/0.5	35
5	BA	2.18	HDDA	16.8	50/1/0.45/0.5	35
6	BA	2.24	BEDA	5.0	50/1/0.45/0.5	35
7	BA	1.64	BEDA	5.0	50/1/0.45/0.5	25
8	BA	1.04	BEDA	5.0	50/1/0.45/0.5	15
9	BA	2.26	BEDA	5.0	200/1/0.45/0.5	35

[a] y_C is the mole fraction of diacrylate in the monomers mixture, $y_C = \frac{[CL]}{[CL]+[M]}$.
[b] V_M represents the volume fraction of acrylate monomer in the solution.
[c] Monomer concentration ([M]) expressed in mol/dm^3.

Table 2.
Description of a set of experiments performed in the study of the FRP copolymerization of Acrylate/Diacrylate monomers at 60 °C.

Run	M	[M]	CL	y_C (%)	[I]	V_M (%)
1	BA	1.05	–	0.0	2.75×10^{-3}	15
2	BA	1.05	HDDA	0.02	2.75×10^{-3}	15
3	BA	1.05	HDDA	0.5	2.76×10^{-3}	15
4	BA	1.04	HDDA	2.1	2.74×10^{-3}	15
5	BA	1.04	HDDA	4.1	2.75×10^{-3}	15
6	BA	2.44	–	0.0	2.74×10^{-3}	35
7	BA	2.43	HDDA	0.5	2.73×10^{-3}	35
8	BA	2.41	HDDA	2.0	2.71×10^{-3}	35

[a] Monomer and initiator concentrations ([M] and [I]) expressed in mol/dm^3.

temperature of 30 °C and using THF as the eluent at 1 mL/min flow rate. A Wyatt Technology OPTILAB DSP 633 nm interferometric refractometer was used to measure the refractive index increment (dn/dc) for the polymers, solvents and monomers in THF, required for analyzing the MALLS results and for estimating the conversion from the values of the differential refractometer (RI) peak areas of monomers and polymer in the chromatographic traces of the SEC analysis. The accuracy of this method has been confirmed by gravimetry.

Kinetic Modeling of FRP and ATRP Acrylate/Diacrylate Copolymerization

Prediction of molecular size distributions, sequence size distributions and z-average radius of gyration for non-linear polymerizations is possible before and after gelation (if needed) using a general kinetic approach.[6–9] These recent developments are based on work developed in the early nineties.[10] Generating functions (GF) of the rate of change of polymer species by chemical reactions ($G_{\mathcal{R}_P}$, $G_{\mathcal{R}_S}$ and $G_{\mathcal{R}_{Hn}}$) can be obtained for general kinetic schemes and the insertion of these GF in the population balance equations (PBE) of a non-steady state perfectly mixed continuous stirred tank reactor (CSTR) yields PBE in terms of the GF of size distributions of mole concentrations of polymer species, sequences and pendent chains (named $G(\mathbf{s})$, $U(\mathbf{s})$ and $G_n^H(\mathbf{s}^-, \mathbf{s}^+)$, respectively):

$$\frac{\partial G}{\partial t} = G_{\mathcal{R}_P} + \frac{G_F(t) - G}{\tau} - \mathcal{R}_v G; \qquad G_{|t=0} = G_0[\mathbf{s_0}(t, \mathbf{s})] \tag{1}$$

$$\frac{\partial U}{\partial t} = G_{\mathcal{R}_S} + \frac{U_F(t) - U}{\tau} - \mathcal{R}_v U; \qquad U_{|t=0} = U_0[\mathbf{s_0}(t, \mathbf{s})] \tag{2}$$

$$\frac{\partial G_n^H}{\partial t} = G_{\mathcal{R}_{Hn}} + \frac{G_{nF}^H(t) - G_n^H}{\tau} - \mathcal{R}_v G_n^H; \qquad G_{n|t=0}^H = G_{n0}^H\left[\mathbf{s_0^-}(t, \mathbf{s}^-), \mathbf{s_0^+}(t, \mathbf{s}^+)\right] \tag{3}$$

Note that $G_{\mathcal{R}_P}$, $G_{\mathcal{R}_S}$ and $G_{\mathcal{R}_{Hn}}$ express the influence of the kinetics on the change of polymer degrees of polymerization, sequences and z-average radius of gyration, respectively. In batch reactor without volume change, right hand sides of Eqs. (1)-(3) only include these contributions of which detailed expressions were derived elsewhere.[6–10] PBEs represented by Eqs. (1)-(3) are non-linear first order partial differential equations that can be solved by the method of the characteristics.[6–10] Batch, plug flow and semi-batch reactors are special cases of a CSTR and, owing to their generality, master equations Eqs. (1)-(3) can be applied in an automated way (numerical approach is preferable as no analytical solution exists for most problems) to different polymerization systems and reactors involving branching (e.g. involving transfer to polymer and/or terminal branching[11,12]) and/or crosslinking of multifunctional monomers.

Several complexities of non-linear polymerizations can be tackled by this method, which is also free of several approximations of non-universal applicability. Existence of multiple kinds of radicals and double bonds are examples of complexities that can be easily taken into account with this approach. Use of simplified statistical approaches, quasi-steady state for radical concentrations, closure conditions for the moments, absence of multiple radical centers in the same molecule are some approximations used in alternative methods

that are also avoided by this general kinetic modeling. A crucial issue which avoids several simplifying assumptions often used with earlier models of non-linear radical polymerizations stems from allowing that all polymer molecules containing radical sites or devoid of them (*dead* species) engage in the same reactions. Important deleterious effects in the quality of predictions can result from the cumulative use of these simplifications; for instance, the spurious prediction of gelation (not experimentally observed) for CSTR polymerizations involving long-chain branching but no combination. Other distinctive features of this approach as compared to alternative methods can be found in the aforementioned works.[6–9,11,12]

These theoretical concepts have been recently applied to the modeling of FRP copolymerization of methyl methacrylate (MMA) with ethylene glycol dimethacrylate (EGDMA) in a batch reactor[13] and styrene (S) with divinylbenzene (DVB) in a semi-batch reactor.[5]ATRP of MMA/EGDMA and NMRP of S/DVB were also recently studied using this approach.[14]

In the present work, a kinetic scheme comprising a total of 28 different chemical groups was considered in modeling studies of the FRP with acrylate/diacrylate:

- Different kinds of polymer radicals (9)
- Different kinds of macromonomers, namely, pendent double bonds (from diacrylate monomer), terminal double bonds (from termination by disproportionation and chain transfer to monomer) and H and CH_3 chain transfer to polymer centers (5)
- Reactants and primary radicals (6)
- Polymer structural units (e.g. repeating units, branching/crosslinking points) (8)

In modeling studies of ATRP with acrylate/diacrylate a kinetic scheme involving a total of 40 different chemical groups was considered:

- Different kinds of growing polymer radicals (9)
- Different kinds of dormant polymer radicals (9)
- Different kinds of macromonomers as described in the FRP case study (5)
- Reactants (e.g. monomers, initiator, transition metal site) and primary radicals (9)
- Polymer structural units (8)

A set of 175 different chemical reactions was considered in the kinetic scheme of FRP acrylate/diacrylate which can be classified as follows:

- Initiator decomposition (1)
- Initiations (20)
- Propagations of different kinds of macromonomers (35)
- Intermolecular chain transfers to polymer (14)
- Chain transfers to monomers and solvent (21)
- Terminations by combination and disproportionation (84)

ATRP acrylate/diacrylate modeling studies were performed by considering a kinetic scheme with 196 different chemical reactions:

- Reversible activation/deactivation of initiator (2)
- Initiations (20)
- Propagations of different kinds of macromonomers (35)
- Intermolecular chain transfers to polymer (14)
- Chain transfers to monomers and solvent (21)
- Terminations by combination and disproportionation (84)
- Reversible activation/deactivation of growing radicals (18)
- Reversible activation/deactivation of primary radicals (2)

For both polymerization systems, much more complex kinetic schemes result if intramolecular chain transfer to polymer (backbiting) and/or β-scission reactions[15–17] are also taken into account. These phenomena were not considered in the present

work. Branching mechanisms (intramolecular/intermolecular) in acrylates polymerization should be specially important at high temperatures (e.g. in the range 75 to 100 °C) and at high polymer concentration (e.g. emulsion/suspension polymerization at high monomer conversion) leading eventually to gelation.[18,19] Simulations here performed, considering the polymerization conditions experimentally used, show that the contribution of intermolecular chain transfer to polymer to the formation of non-linear connections is negligible as compared with the main crosslinking process.

Modeling studies of FRP and ATRP acrylate/diacrylate were carried out considering basic sets of rate coefficients collected from previous works (see also (3)), namely for initiator thermal decomposition,[20] *n*BA propagation,[21] chain transfer to monomer,[22] chain transfer to solvent,[20,23] intramolecular chain transfer to polymer,[24] termination.[23,25] Rate coefficients for reversible kinetic steps of ATRP, namely, radical activation, radical deactivation or equilibrium constant activation/deactivation, measured/estimated in previous works,[26–28] were also here considered. Sensitivity analysis of the branching and crosslinking processes to kinetic parameters was performed by considering perturbations of the rate coefficients governing different reaction steps, namely: propagation of pendent double bonds, propagation of the different kinds of terminal double bonds, intermolecular chain transfer to different polymer centers, reactivity of the different kinds of polymer radicals and probabilities of radical termination by combination/disproportionation. Under the experimental conditions here used, simulation results show a particular sensitivity to the reactivity of pendent double bonds of diacrylate monomer and therefore only this parameter was used in the fitting of experimental results, as discussed below.

Past experimental/theoretical works using the same simulation method[5,13,14] considered the effect of inhibition/retardation reactions in FRP and CRP polymerization process. Kinetic models accounting for the presence of an inhibitor and/or a retarder in the polymerization system were developed and it was concluded that, for those experimental conditions, the effect of inhibition on average molecular weights should only be noticeable above around 500 ppm. Results thus obtained showed that this possible issue was avoided with the monomers and experimental set-up used. Transient behavior (before and after AIBN addition) due to thermal initiation in styrene/divinylbenzene FRP and NMRP was also simulated and experimentally studied[14] in the framework of the present approach showing the ability to deal with

Table 3.
Basic set of rate coefficients considered in the modeling studies of the FRP and ATRP copolymerization of acrylate/diacrylate monomers.

Kinetic step	Rate coefficient expression	Ref.
Initiator thermal decomposition	$k_d = 4.31 \times 10^{15} \exp(-131.7 \times 10^3/RT)(S^{-1})$, $f = 0.6$	[20]
BA propagation	$k_p = 2.21 \times 10^7 \exp(-17.9 \times 10^3/RT)$	[21]
Initiation by primary radicals	$k_i = k_p$	
Chain transfer to monomer (BA)	$k_{fM} = 2.9 \times 10^5 \exp(-32.6 \times 10^3/RT)$	[22]
Chain transfer to solvent	$C_S = k_{fS}/k_p = 2.7 \times 10^{-4}$	[20]
Intramolecular chain transfer to polymer	$10^{-5} < C_p = k_{fP}/k_p < 10^{-3}$	[24]
Radical termination	$k_p/\sqrt{k_t} = 0.15 + 0.4[M]$	[23]
Combination/Disproportionation	$\alpha_{td} = k_{td}/k_t = 0.05$, $\alpha_{tc} = k_{tc}/k_t = 0.95$	[20]
Equilibrium constant (ATRP)	$K_{ATRP} = k_a/k_{da} = 3.27 \times 10^{-8}$	[28]
Radical deactivation (ATRP)	$k_{da} = 6.1 \times 10^6$	[27]
Propagation of pendent double bonds	$r = k_p^*/k_p$	a)

Kinetic parameters expressed in $dm^3\,mol^{-1}\,s^{-1}$, unless otherwise stated.
$R = 8.314\,J mol^{-1}\,K^{-1}$
[a)] Fitting parameter in this work.

these complexities and were not observed noticeable induction periods. Similar conclusions concerning the importance of the induction period were obtained with the present chemical system. Note that the high proportion initiator/monomer used (namely in ATRP experiments) makes this issue negligible.

Before gelation, as it is the case of the work here performed, our simulation method[6–10] transforms the resolution of partial differential equations (PDE), through the method of the characteristics, into initial value problems (IVP) of systems of ordinary differential equations with conditions at the initial value of the independent variable (polymerization time). Two point boundary value problems (2PBVP) will arise if generic values of generating functions are sought, as for obtaining predictions of size distributions by the numerical inversion of their GF or for computing non-integer moments or moments after gelation. Successive derivation of GF and resolution of the resulting PDE by the method of the characteristics also leads to systems of ODE for the moments up to the prescribed order. The dimension of the system to be solved depends on the complexity of the kinetic scheme involved, namely of the number of different chemical groups and reactions. For instance, to obtain moments up to second order, a system of $N_{eq} = N_A + N_P + N_P(N_P+1)/2 + 1$ ODE must be solved with N_A being the count of active chemical groups and N_P the set of polymer chemical groups considered (active and non-active). The present FRP case study was treated considering $N_A = 20$ and $N_P = 22$ and therefore a system of $N_{eq} = 296$ ODE had to be solved. Note that for this polymerization system 6 chemical groups (e.g. monomers, initiator...) are active but do not belong to the polymer. The same purpose is achieved with $N_{eq} = 560$ ODE for the ATRP system here considered (simulations performed with $N_A = 32, N_P = 31$ and 9 chemical groups not belonging to the polymer). The calculation of the *z*-Average Radius of Gyration in the Θ state ($\overline{R}_{g\theta}$) involves the resolution of IVP with 780 ODE for the FRP system and 1521 ODE with the ATRP case study. The simulations below presented were obtained through the numerical resolution of those problems, using the stiff ODE integrator RADAU5[29].

Unperturbed Dimensions and Prediction of the *z*-Average Radius of Gyration in a Good Solvent

Several effects are involved in the short-range interactions leading to increased molecular size of linear random-coil polymers. The restriction to fixed bond angles expands the polymer chains. Molecular dimensions are further increased due to restricted rotations resulting from steric hindrances or due to rigid planar conformations (e.g. presence of aromatic rings in the main chain). Conformations which would place too close pairs of atoms in neighbor repeating units along the polymer chain are also forbidden. The mean square distance between chain ends including short-range interactions (r_θ^2 - unperturbed dimensions in the absence of long-range interactions) divided by the square of the random-flight end-to-end distance (r_f^2) defines the characteristic ratio C_∞:

$$C_\infty = \lim_{n\to\infty}\left(\frac{r_\theta^2}{r_f^2}\right) = \lim_{n\to\infty}\left(\frac{6R_{g\theta}^2}{nl^2}\right) = \lim_{n\to\infty}\left(\frac{6M}{nl^2}\frac{R_{g\theta}^2}{M}\right) = \frac{6M_0}{2l^2}\frac{R_{g\theta}^2}{M} \qquad (4)$$

with n representing the number of (equal) skeletal bonds of the polymer chain of molecular weight M, M_0 being the molecular weight of the repetitive unit bearing two C−C bonds of length $l = 0.154$ nm. For random coil chains the unperturbed value of the mean square end to end distance (r_θ^2) is related with the unperturbed (Θ conditions) value of the mean square radius of gyration by $r_\theta^2 = 6R_{g\theta}^2$.

The Θ dimensions of linear polymers can be estimated from experimental measurements performed in a good solvent using a SEC/RI/MALLS system.[30,31] For polymer

chains in a good solvent with dimensions greater than $\lambda/20$, with λ being the wavelength of the incident light, the mean square radius of gyration can be measured for each slice of elution volume (considered as monodisperse samples) in a SEC/RI/MALLS apparatus. With the instrument used in this work and operating with THF, the lower detection limit is around $\lambda/20 \simeq \lambda_0/(20 \times n_{THF}) = 658/(20 \times 1.4) = 23.5$ nm. Measurements below this limit are possible (e.g. 10 nm) but with high associated uncertainty (e.g. errors in the order of 50%). Figures 2 (a) and 2(b) show measured variations of molecular weight (M) and of root mean square radius of gyration (R_g) along the SEC trace of a P*n*BA sample synthesized in this work. Observed light scattering (90°) and RI signals are also shown in these figures. In this analysis, the head and tail regions of the chromatograms were eliminated due to their very low LS and RI signals, which would also cause high errors in the estimation of M and R_g. The following average properties of this sample were measured:

$\overline{M}_n \times 10^{-5} = 2.0 \pm 0.1$,
$\overline{M}_w \times 10^{-5} = 3.0 \pm 0.1$,
$\overline{M}_z \times 10^{-5} = 4.2 \pm 0.7$, $\overline{R}_g = 32 \pm 1$ nm.

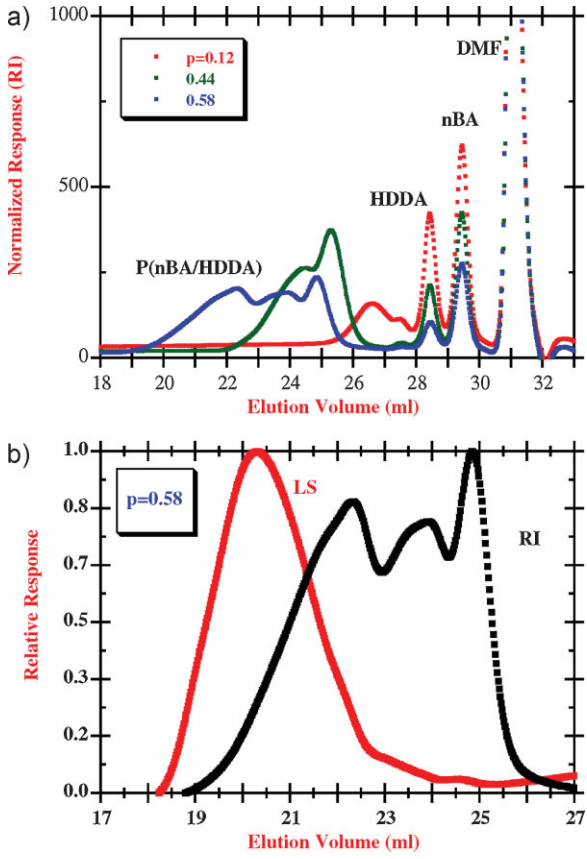

Figure 1.
(a) Observed refractive index signal in the SEC traces of ATRP synthesized Acrylate/Diacrylate copolymers corresponding to different polymerization times (monomer conversion) showing the consumption of monomers and the evolution of the crosslinking process. (b) Measured refractive index and light scattering (90°) signals in the SEC trace of an ATRP synthesized Acrylate/Diacrylate copolymer showing the formation of a cluster of high molecular weight at a low concentration.

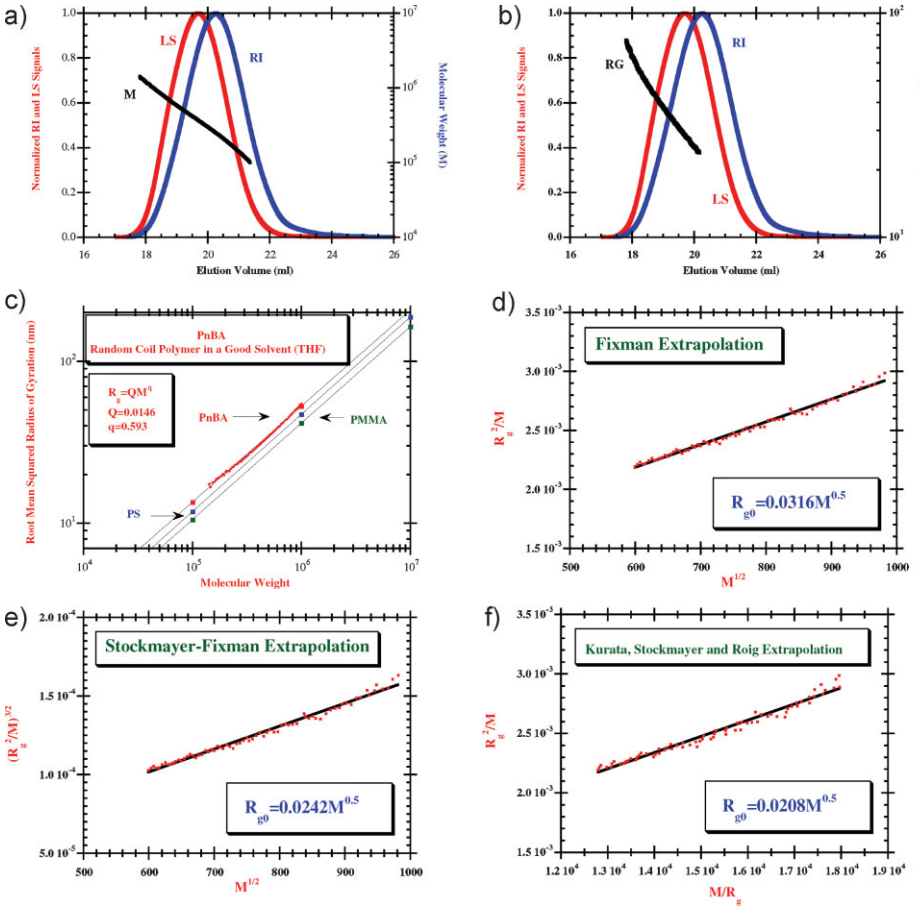

Figure 2.
(a) Measured relation of molecular weight *versus* elution volume in the SEC trace of a FRP synthesized P*n*BA sample. (b) Measured relation of root mean square radius of gyration *versus* elution volume for the same P*n*BA sample of (a). (c) Scaling law for the radius of gyration *versus* molecular weight observed for P*n*BA in a good solvent and its comparison with scaling laws measured for the dimensions of other polymers. (d) Estimated unperturbed dimensions of P*n*BA considering Fixman extrapolation. (e) Estimated Θ dimensions of P*n*BA with Stockmayer-Fixman extrapolation. (f) Estimated Θ dimensions of P*n*BA with Kurata-Stockmayer-Roig extrapolation.

Measured values of M and R_g along the chromatogram of the P*n*BA sample were used to establish a relation R_g *versus* M which is known to follow a scaling law of the form $R_g = QM^q$. Figure 2(c) shows the scaling law $R_g = 0.0146M^{0.593}$ that was estimated in this work for P*n*BA in THF at 30 °C. This result is consistent with measurements reported in other research works using other polymers, namely $R_g = 0.011M^{0.596}$ for PMMA[32] in THF at 30 °C and $R_g = 0.0118M^{0.6}$ for PS[33] in THF at 25 °C that are also presented in Figure 2(c).

Experimental values expressing the dependence of the dimensions of P*n*BA in THF on molecular weight were used to estimate the unperturbed dimensions of this polymer. Different extrapolation procedures were used for this purpose:

Fixman[34] extrapolation:

$$\frac{R_g^2}{M} = \frac{R_{g\theta}^2}{M} + 0.0299B\left(\frac{R_{g\theta}^2}{M}\right)^{-1/2} M^{1/2} \quad (5)$$

Stockmayer-Fixman[35] extrapolation:

$$\left(\frac{R_g^2}{M}\right)^{3/2} = \left(\frac{R_{g\theta}^2}{M}\right)^{3/2}\left(1 + CM^{1/2}\right) \quad (6)$$

Kurata-Stockmayer-Roig[36] extrapolation:

$$\frac{R_g^2}{M} = \frac{R_{g\theta}^2}{M} + 0.0286Bg(\alpha)\left(\frac{M}{R_g}\right) \quad (7)$$

The application of these extrapolation procedures to the synthesized P*n*BA sample is shown in Figures 2(d)-(f). Good agreement between experimental values and theoretical predictions are obtained with the three different methods. Extrapolated unperturbed dimensions of P*n*BA are closer when Stockmayer-Fixman or Kurata-Stockmayer-Roig extrapolations are used and higher dimensions are estimated with Fixman extrapolation. Characteristic ratios $C_\infty = \frac{3\times128\times0.0208^2}{0.154^2} = 7.0$, $C_\infty = 9.5$ and $C_\infty = 16.2$ are estimated when Kurata-Stockmayer-Roig, Stockmayer-Fixman and Fixman extrapolation results are considered, respectively. The length of a C–C bond, $l = 0.154$ nm was here considered.

Experimental studies concerning the polymer chain flexibility of polyacrylic esters,[37,38] report (among others) the length of the Kuhn segment for P*n*BA: $A_m = 6\frac{R_{g\theta}^2}{M}\frac{M_0}{b_0} = 3.54$ nm, with b_0 representing the contribution of each monomeric unit to the length of the polymer chain ($b_0 = 0.211$ nm was considered in these works[37,38] for polyacrylates). This definition is generically consistent with Eq. (4) if the relation $b_0^2 = 2l^2$ is considered. These experimental results can be used to estimate the characteristic ratio of P*n*BA because its relation with Kuhn's statistical segment is expressed by $C_\infty = \frac{\sqrt{2}A_m}{2l}$ and therefore $C_\infty = 16.3$ results for P*n*BA. Based on these same works, $C_\infty = 9.3$ ($A_m = 2.02$ nm) can be estimated for PMA. Other experimental/theoretical studies[39] estimate $C_\infty = 8.4$ for PMA. It is well known that the structure of polymer chains plays a strong influence on the polymer chain flexibity. For polymethacrylates the effect of the substituent on the chain flexibility was thoroughly studied and values of C_∞ are reported[40] to lie between 7.3 (methyl methacrylate) and 26.4 (pentachlorophenyl methacrylate). For *n*-butyl methacrylate (P*n*BMA) the characteristic ratio was experimentally evaluated and theoretically predicted[40,41] to be in the range 8.6 to 9.6. Chain flexibility of polymethacrylates has been extensively studied but for polyacrylates only few research works are available. Characteristic ratio of poly(tetrahydrofurfuryl acrylate) and poly(2-ethylbutyl acrylate) were more recently measured and $C_\infty = 8.6$ and 9.2, respectively, have been reported.[42] Based on the available range values of the characteristic ratio of PMMA, PMA, P*n*BMA and on the effect of substitution groups, a value around 10 is expected for P*n*BA. The measurement of C_∞ around 16 before reported for P*n*BA,[37,38] and also obtained in the present work when Fixman extrapolation is considered, seems to be overestimated.

Similarly to other works dealing with estimation of unperturbed dimensions of polymer chains considering different extrapolation methods,[30,31,38] in the present work, the mean of the three extrapolations for the unperturbed dimensions of P*n*BA will be used: $R_{g\theta} = 0.0255M^{0.5}$. This estimate leads to a characteristic ratio $C_\infty = 10.5$ and a Kuhn segment of length $A_m = 2.29$ nm. Note that an imaginary bond length (b) connecting a set of beads (repeating units) in the context of the freely rotating model can be calculated because the following relation holds: $b^2 = A_m b_0 = \sqrt{2}A_m l$. Therefore, in the predictions of the *z*-average radius of gyration performed in the present work, a bond length of $b = 0.706$ nm was considered to link *n*BA repeating units.

Using the experimentally observed relation $R_g = 0.0146M^{0.593}$ for P*n*BA in THF at 30 °C and the extrapolation $R_{g\theta} = 0.0255M^{0.5}$ estimated for a Θ solvent, we estimate that also in THF at 30 °C, for polydispersed P*n*BA, the following expansion relation holds: $\overline{R}_g/\overline{R}_{g\theta} = 0.573\overline{M}_z^{0.093}$. Our simulation method is able to estimate the *z*-Average Radius of Gyration in the Θ state ($\overline{R}_{g\theta}$) but experimental measurements were performed in THF at 30 °C (good solvent regimen). Predictions of $\overline{R}_g$ are therefore needed and this expansion relation was used with this purpose in the present work. This same expansion relation was considered in the linear and non-linear polymerization systems, as described below.

Results and Discussion

Figure 3(a) shows measured and predicted monomer conversion evolutions of $\overline{M}_w$ in FRP *n*BA/HDDA copolymerizations, at 15% initial volume fraction of monomer ($V_M = 15\%$), with different mole fractions of crosslinker, showing the strong influence of the initial amount of HDDA in the dynamics of polymer properties. These experiments were simulated using the reactivity of PDBs as fitting parameters. It was estimated that PDBs present a lower reactivity as compared to *n*BA, with a ratio of propagation constants $r = k_p^*/k_p = 0.06$. Simulation results have shown a low sensitivity to changes in other kinetic parameters besides the reactivity of PDB. Reactivities of the different kinds of polymer radicals have a small effect on the branching/crosslinking process only if they are very low as compared with the reactivity of the radical correspondent to the acrylate monomer (e.g. below 1/1000). Simulations also have shown that, under the polymerization conditions here considered, the branching process due to intermolecular chain transfer to polymer (H and CH_3 chain transfer centers were considered) have a negligible contribution to the formation of non-linear architectures, namely when compared with the crosslinking phenomena. Reactivity ratios for intermolecular chain transfer to polymer in the range $10^{-5} < C_P = k_{fP}/k_p < 10^{-3}$ are reported in the literature[24] and simulations have shown a very small impact of this mechanism on the polymer properties only when the upper limit of this interval is approached and the mole fraction of diacrylate monomer is very small (e.g. y_C below 0.5%). Note that chain transfer to solvent ($C_S = k_{fS}/k_p = 2.7 \times 10^{-4}$) is here an important competitive mechanism as compared with chain transfer to polymer.[11,12] Similar conclusions were obtained with respect to the impact of polymerization of terminal double bonds. Simulations were performed considering that the fraction of termination by combination is 95%.

In Figure 3(b) is presented the effect of the monomer dilution (experiments with $V_M = 15\%$ and $V_M = 35\%$) in the evolution of $\overline{M}_w$ for *n*BA/HDDA FRP copolymerizations with the same initial mole fraction of diacrylate ($y_C = 0.5\%$). Completely distinct evolutions of $\overline{M}_w$ with monomer conversion were experimentally measured and different values for the reactivity of PDBs are fitted from these two experiments: $r = k_p^*/k_p = 0.16$ for $V_M = 35\%$ and $r = 0.06$ for $V_M = 15\%$. It is plausible that these reactivity ratios are only apparent values due to the influence of intramolecular cyclization reactions which had been neglected in these modeling studies. Increased deviation from the ideal case ($r = k_p^*/k_p = 1$) with dilution seems to confirm this issue.

In Figure 3(c) are compared FRP and ATRP *n*BA/HDDA copolymerizations with the same initial dilution ($V_M = 35\%$) and the same amount of crosslinker ($y_C = 2\%$). Experimental results and simulations show the distinct behavior of the crosslinking process when FRP and ATRP synthesis techniques are used. In fact, ATRP can be used at least to have a better control on the dynamics of gelation of acrylate/diacrylate polymerization systems. Operation at higher contents of crosslinker

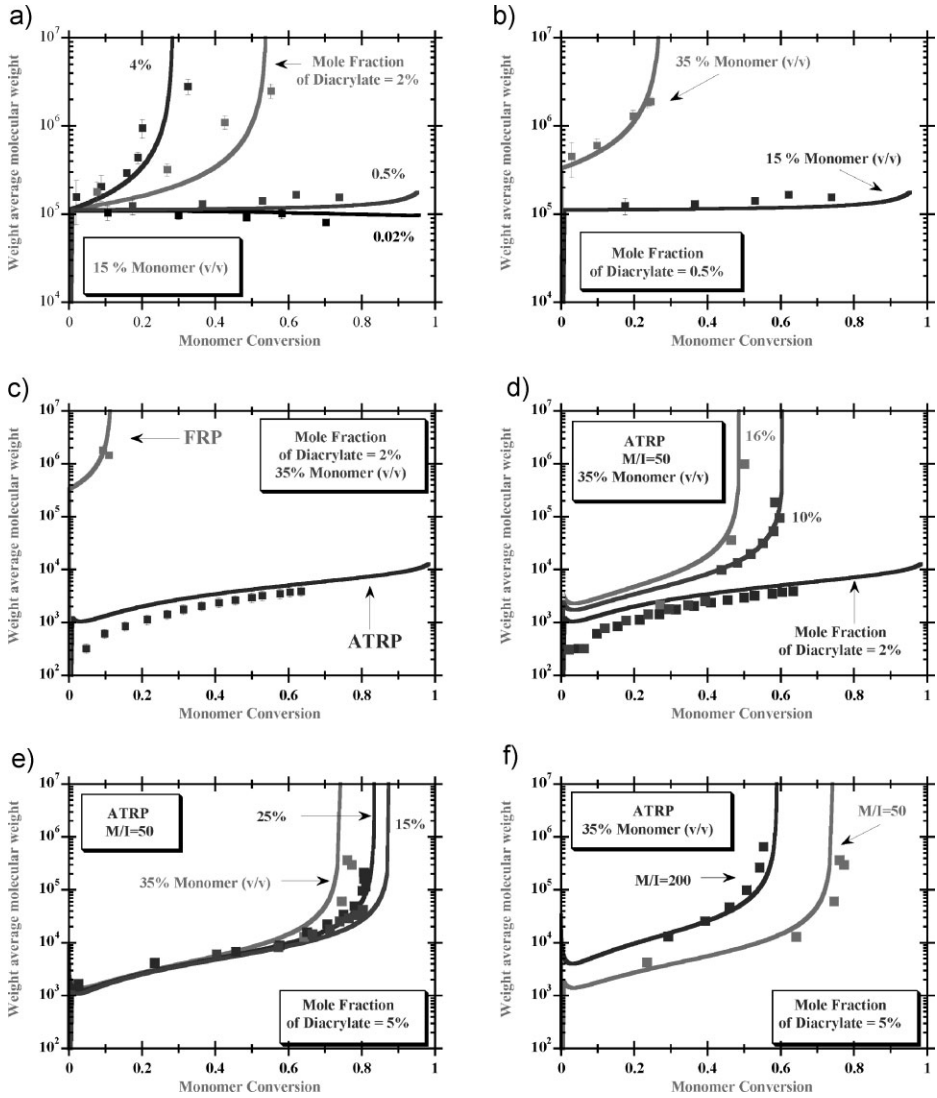

Figure 3.
(a) Measured and predicted evolution of $\overline{M}_w$ in *n*BA/HDDA FRP copolymerization with different initial amounts of diacrylate ($V_m = 15\%$). (b) Effect of the dilution in the evolution of $\overline{M}_w$ for FRP copolymerization of *n*BA/HDDA. (c) Comparison of FRP and ATRP copolymerizations of *n*BA/HDDA with the same initial dilution and amount of crosslinker. (d) Effect of the initial amount of crosslinker in the evolution of $\overline{M}_w$ for ATRP copolymerization of *n*BA/HDDA. (e) Effect of the dilution in ATRP of *n*BA/BEDA. (f) Effect of the initial ratio Monomer/Initiator in ATRP of *n*BA/BEDA.

without gelation is possible with ATRP when compared with FRP and this is an important issue in the production of hyperbranched polymers.

The effect of the initial amount of crosslinker in the evolution of $\overline{M}_w$ for ATRP *n*BA/HDDA copolymerization at constant initial dilution ($V_M = 35\%$) is presented in Figure 3(d). Experimental results were used to fit the reactivity ratio of PDB and the value $r = 0.3$ was obtained. Note that simulations with the ATRP case study also have confirmed the negligible impact (at least with the operation conditions here considered) of intermolecular chain transfer to polymer and polymerization of

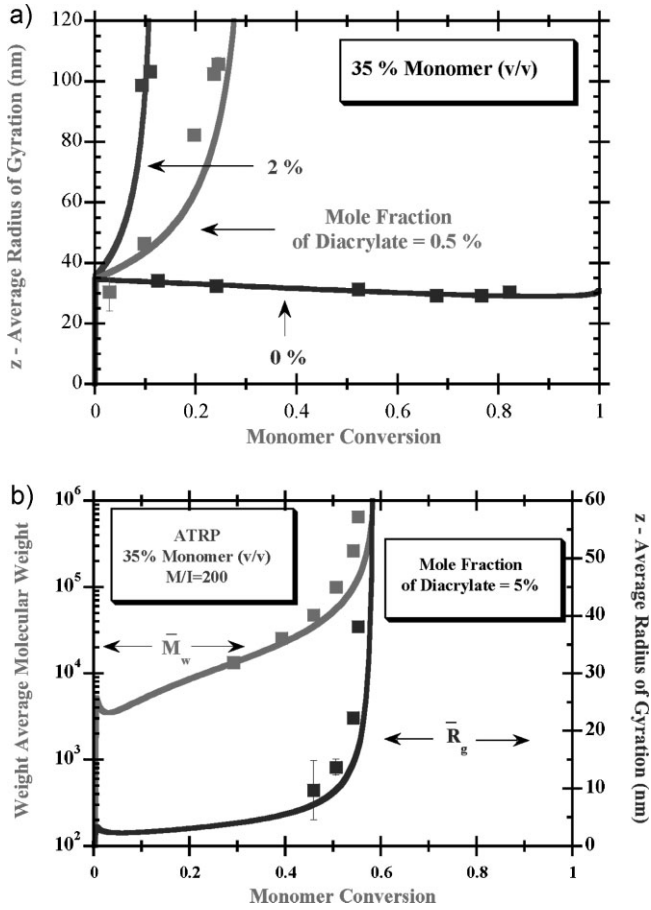

Figure 4.
(a) Measured and predicted evolution of $\overline{R}_g$ in FRP homopolymerization of *n*BA and *n*BA/HDDA copolymerization with different amounts of diacrylate. (b) Measured and predicted evolution of $\overline{R}_g$ and $\overline{M}_w$ in *n*BA/BEDA ATRP copolymerization with initial mole fraction of diacrylate $y_C = 5\%$ and $M/I = 200$.

terminal double bonds, when compared with the crosslinking process. Estimated values of the reactivity ratios of PDB for ATRP process are also apparent due to the effect of intramolecular cyclizations. Nevertheless, at the same initial dilution, the estimated reactivity of PDB in ATRP ($r = 0.3$) is higher than in FRP ($r = 0.16$). It is plausible that this difference is due to the lower magnitude of intramolecular cyclizations in ATRP which can be an important advantage for the production of more homogeneous networks.

Figure 3(e) shows the effect of the monomer dilution in the ATRP of *n*BA/BEDA copolymerizations at constant initial mole fraction of diacrylate ($y_C = 5\%$). These results confirm the importance of the intramolecular cyclizations reactions, even in ATRP. Estimated reactivity ratios of $r = 0.3$, 0.2 and 0.17 at $V_M = 35\%$, 25% and 15%, respectively, show the increasing importance if this mechanism at higher dilutions. In Figure 3(f) is shown that the initial molar ratio between monomer and initiator (M/I) can also be used, trough the manipulation of the length of the primary chain, to control the crosslinking process and therefore to help in the production of tailored hyperbranched polymers.

Measured and predicted evolution of the *z*-average radius of gyration ($\overline{R}_g$) for FRP

acrylate/diacrylate copolymerizations performed with different amounts of diacrylate are presented in Figure 4(a). Calculations of $\overline{R}_g$ have been carried out using the same set of kinetic parameters as in the calculations of molecular weights. Despite the huge simplifications above discussed which were used in the prediction of $\overline{R}_g$, a good agreement between experimental observations and predictions is obtained with different polymerization conditions. Figure 4(b) shows predicted and observed monomer conversion evolution of $\overline{R}_g$ and $\overline{M}_w$ in *n*BA/BEDA ATRP copolymerization with initial mole fraction of diacrylate $y_C = 5\%$ and $M/I = 200$. A simultaneous good agreement between measurements and predictions of average molecular weights and *z*-average radius of gyration is observed, confirming this general kinetic approach as a valuable tool to predict and design some important features of the molecular architecture of such complex materials.

Conclusions

In this work, the molecular architecture of FRP and ATRP synthesized polyacrylate hyperbranched polymers and networks was experimentally and theoretically studied. Such non-linear polymers were synthesized at 1 dm^3 scale and the dynamics of formation of products was characterized by SEC/RI/MALLS. In the framework of a general kinetic approach, for both polymerization systems, models were developed taking into account the polymerization of different kind of macromonomers (pendent double bonds, terminal double bonds and chain transfer to polymer centers) and the existence of different kinds of polymer radicals. The most important conclusions are as follows:

- Under the experimental/theoretical conditions here considered, namely low temperature (60 °C) and low monomer concentration (e.g. 35% v/v), the impact of branching processes (intermolecular chain transfer to polymer, polymerization of terminal double bonds) in the molecular architecture of acrylate/diacrylate copolymers is very low as compared with the main crosslinking process (polymerization of pendent double bonds).
- Experimental results at different monomer dilutions put into evidence the important effect of intramolecular reactions (cyclizations) on the molecular architecture of these microgels. These reactions should be minimized if microgels with improved homogeneity are desired.
- Important differences were observed in the molecular architecture of non-linear products synthesized either by FRP or by ATRP. Improved microgel homogeneity can be obtained by ATRP of acrylate/diacrylate monomers. Comparatively to FRP, ATRP also allows the operation with higher crosslinker mole fraction without gel production. These results can be especially useful to obtain hyperbranched polymers at higher conversions than with FRP.

Additional theoretical developments accounting for cyclization reactions are needed but the aforementioned comparative studies are the key for carrying out a quantitative modeling of loop formation for these chemical systems. Suspension polymerization leading to gel formation can also be used to elucidate the importance of these mechanisms in network production. Ongoing research concerning the *in-line* monitoring of these polymerization systems by FTIR-ATR should eventually lead to further important informations about the reactivity of pendent double bonds and the branching/crosslinking processes.

Notation

A_m	length of Kuhn's statistical segment of polymer chain.
B	parameter in Fixman (Eq. (5)) and Kurata-Stockmayer-Roig (Eq. (7)) extrapolations.

b_0	contribution of monomeric units to the length of polymer chains.
C	parameter in Stockmayer-Fixman (Eq. (6)) extrapolation.
C_∞	characteristic ratio.
$C_P = k_{fP}/k_p$	reactivity ratio for intermolecular chain transfer to polymer.
$C_S = k_{fS}/k_p$	reactivity ratio for chain transfer to solvent.
f	thermal initiator decomposition efficiency.
$g(\alpha)$	function in Kurata-Stockmayer-Roig (Eq. (7)) extrapolation.
$G(\mathbf{s})$	generating function of the distribution of mole concentrations of polymer species according to their counts of chemical groups (also known as the size distribution of polymer species concentrations).
$G_n^H(\mathbf{s}^+, \mathbf{s}^-)$	generating function of the size distribution of pendent chains.
G_{RH_n}	generating function of the rate of change of the size distribution of polymer pendent chains by chemical reactions.
$G_{\mathcal{R}_P}$	generating function of the rate of change of the size distribution of polymer species by chemical reaction.
$G_{\mathcal{R}_S}$	generating function of the rate of change of the size distribution of polymer sequences by chemical reaction.
[I]	initiator concentration (mol/dm^3).
k_a	rate coefficient of radical activation in ATRP.
k_{da}	rate coefficient of radical deactivation in ATRP.
k_d	rate coefficient of the unimolecular thermal initiator decomposition.
k_{fM}	rate coefficient of the chain transfer to monomer.
k_{fP}	rate coefficient of the intermolecular chain transfer to polymer.
k_{fS}	rate coefficient of the chain transfer to solvent.
k_p	rate coefficient of the propagation of vinyl monomer.
k_p^*	rate coefficient of the propagation of pendent double bonds.
k_t	rate coefficient of the global radical termination.
k_{tc}	rate coefficient of the radical termination by combination.
k_{td}	rate coefficient of the radical termination by disproportionation.
$K_{ATRP} = k_a/k_{da}$	equilibrium constant for radical activation/deactivation (ATRP).
l	bond length (0.154 nm for C–C bonds).
M	polymer chain molecular weight.
M_0	molecular weight of a repetitive unit.
$[M]$	monomer concentration (mol/dm^3).
$\overline{M}_n$	number-average relative molecular mass.
$\overline{M}_w$	weight-average relative molecular mass.
$\overline{M}_z$	z-average relative molecular mass.
N_{eq}	dimension of the system of ODE to be solved.
N_A	number of different kinds of active chemical groups (including special individual molecules, like monomers and initiators) considered in the polymerization system.
N_P	number of different kinds of chemical groups considered in polymer molecules

	(active and non-active groups).
$r = k_p^*/k_p$	reactivity ratio for the propagation of pendent double bonds.
r_f^2	square of the random-flight end-to-end distance.
r_θ^2	unperturbed polymer dimensions in the absence of long-range interactions.
R	ideal gas constant ($R = 8.314$ Jmol^{-1}K^{-1}).
R_g	root mean square radius of gyration.
$R_{g\theta}$	unperturbed (Θ) root mean square radius of gyration.
$\overline{R}_g$	root z-average mean square radius of gyration.
$\overline{R}_{g\theta}$	unperturbed root z-average mean square radius of gyration.
R_v	relative rate of change of volume caused by chemical reaction.
$\mathbf{s}$	vector of dummy Laplace parameters of the generating functions associated with the size distributions (distributions according to the counts of chemical groups) of polymer species or sequences.
$\mathbf{s}^-$, $\mathbf{s}^+$	vectors of dummy Laplace parameters of the generating function associated with the size distributions of the bilateral pendent chains within polymer molecules.
t	time.
T	temperature.
$U(\mathbf{s})$	generating function of size distribution of mole concentrations of polymer sequences.
V_M	volume fraction of vinyl monomer in the solution.
y_C	mole fraction of divinyl monomer in the monomers mixture.

Greek Characters

α_{tc}	fraction of radical termination by combination.
α_{td}	fraction of radical termination by disproportionation.
λ	wavelength of the light (nm).
τ	space time (ratio of reactor volume and inlet volume flow rate).

Subscripts

F	in feed.
n	number average.
w	weight average.
z	average.
0	initial.

Abbreviations

AIBN	2,2′-azobis(2-methylpropionitrile).
ATRP	atom transfer radical polymerization.
BA	*n*-butyl acrylate.
BEDA	bisphenol A ethoxylate diacrylate.
CL	crosslinker.
CRP	controlled radical polymerization.
CSTR	continuous stirred tank reactor.
DMF	*N,N*-dimethylformamide.
DVB	divinylbenzene.
EBrP	ethyl 2-bromopropionate.
EGDMA	ethylene glycol dimethacrylate.
FRP	free radical polymerization.
GF	generating function.
HDDA	1,6-Hexanediol diacrylate.
I	initiator.
M	monomer.
MA	methyl acrylate.
MEHQ	monomethyl ether hydroquinone.

MMA	methyl methacrylate.
MWD	molecular weight distribution.
NMRP	nitroxide-mediated radical polymerization.
ODE	ordinary differential equation.
PBE	population balance equation.
PDB	pendent double bond.
PDE	partial differential equation.
PMDETA	*N,N,N′,N″,N″*-pentamethyldiethylenetriamine.
PMMA	poly(methyl methacrylate).
PMA	poly(methyl acrylate).
P*n*BA	poly(*n*-butyl acrylate).
P*n*BMA	poly(*n*-butyl methacrylate).
PS	polystyrene.
RG	root mean-square radius of gyration.
SEC/RI/MALLS	size exclusion chromatography with refractive index and multi-angle laser light scattering detection.
S	styrene.
THF	tetrahydrofuran.

Acknowledgements: Financial support by Fundação para a Ciência e a Tecnologia (FCT), Ministry of Science and Technology of Portugal and European Community (FEDER) through project POCI-PPCDT/EQU/60483/2004 is gratefully acknowledged.

[1] A. Matsumoto, *Adv. Polym. Sci.* **1995**, *123*, 41.
[2] Q. Yu, M. Zhou, Y. Ding, B. Jiang, S. Zhu, *Polymer* **2007**, *48*, 7058.
[3] H. Gao, K. Min, K. Matyjaszewski, *Macromolecules* **2007**, *40*, 7763.
[4] H. Gao, W. Li, K. Matyjaszewski, *Macromolecules* **2008**, *41*, 2335.
[5] M. A. D. Gonçalves, R. C. S. Dias, M. R. P. F. N. Costa, *Macromol. Symp.* **2007**, *259*, 124.
[6] M. R. P. F. N. Costa, R. C. S. Dias, *Chem. Eng. Sci.* **2005**, *60*, 423.
[7] R. C. S. Dias, M. R. P. F. N. Costa, *Polymer* **2006**, *47*, 6895.
[8] M. R. P. F. N. Costa, R. C. S. Dias, *Polymer* **2007**, *48*, 1785.
[9] R. C. S. Dias, M. R. P. F. N. Costa, *Macromol. React. Eng.* **2007**, *1*, 440.
[10] M. R. P. F. N. Costa, R. C. S. Dias, *Chem. Eng. Sci.* **1994**, *49*, 491.
[11] R. C. S. Dias, M. R. P. F. N. Costa, *Macromolecules* **2003**, *36*, 8853.
[12] R. C. S. Dias, M. R. P. F. N. Costa, *Macromol. Theory Simul.* **2005**, *14*, 243.
[13] I. M. R. Trigo, M. A. D. Gonçalves, R. C. S. Dias, M. R. P. F. N. Costa, *Macromol. Symp.* **2008**, *271*, 107.
[14] M. A. D. Gonçalves, I. M. R. Trigo, R. C. S. Dias, M. R. P. F. N. Costa, Submitted to the Polymer Networks Group Conference Proceedings *Macromol. Symp.* **2008**.
[15] R. A. Hutchinson, A. Penlidis, *Polymer Reaction Engineering*, (Chapter 3) **2007**, Blackwell Publishing.
[16] A. N. Nikitin, R. A. Hutchinson, *Macromolecules* **2005**, *38*, 1581.
[17] A. N. Nikitin, R. A. Hutchinson, M. Buback, P. Hesse, *Macromolecules* **2007**, *40*, 8631.
[18] C. Plessis, G. Arzamendi, J. R. Leiza, H. A. S. Schoonbrood, D. Charmot, J. M. Asua, *Macromolecules* **2000**, *33*, 4.
[19] I. González, J. R. Leiza, J. M. Asua, *Macromolecules* **2006**, *39*, 5015.
[20] G. Moad, D. H. Solomon, *The Chemistry of Radical Polymerization*, **2006**, 2nd Ed., Elsevier, Oxford.
[21] J. M. Asua, S. Beuermann, M. Bubak, P. Castignolles, B. Charleux, R. G. Gilbert, R. A. Hutchinson, J. R. Leiza, A. N. Nikitin, J.-P. Vairon, A. M. van Herk, *Macromol. Chem. Phys.* **2004**, *205*, 2151.
[22] S. Maeder, R. G. Gilbert, *Macromolecules.* **1998**, *31*, 4410.
[23] T. F. McKenna, A. Villanueva, A. M. Santos, *J. Polym. Sci. Part A: Polym. Chem.* **1999**, *37*, 571.
[24] J. Brandrup, E. H. Immergut, E. A. Grulke, *Polymer Handbook*, **1999**, 4th Ed. John Wiley & Sons, New York.
[25] M. Fernández-García, M. Fernández-Sanz, E. L. Madruga, *J. Polym. Sci. Part A: Polym. Chem.* **2004**, *42*, 130.
[26] W. Tang, K. Matyjaszewski, *Macromolecules* **2007**, *40*, 1858.
[27] K. Matyjaszewski, H.-J. Paik, P. Zhou, S. J. Diamantini, *Macromolecules* **2001**, *34*, 5125.
[28] W. Tang, N. V. Tsarevsky, K. Matyjaszewski, *J. Am. Chem. Soc.* **2006**, 1598.
[29] E. Hairer, G. Wanner, *Solving Ordinary Differential Equations II*, **2002**, 2th Ed. Springer, Berlin.
[30] J. Búrdalo, R. Medrano, E. Saiz, M. P. Tarazona, *Polymer* **2000**, *41*, 1615.
[31] M. P. Tarazona, E. Saiz, *J. Biochem. Biophys. Methods* **2003**, *56*, 95.
[32] C. Jackson, Y.-J. Chen, J. W. Mays, *J. Appl. Polym. Sci.* **1996**, *59*, 179.
[33] K. Terao, J. W. Mays, *Eur. Polym. J.* **2004**, *40*, 1623.
[34] M. Fixman, *J. Chem. Phys.* **1955**, *23*, 1656.

[35] W. H. Stockmayer, M. Fixman, *J. Polym. Sci.* **1963**, *C1*, 137.
[36] M. Kurata, W. H. Stockmayer, A. Roig, *J. Chem. Phys.* **1960**, *33*, 151.
[37] E. Penzel, N. Goetz, *Die Angewandte Makromolekulare Chemie* **1990**, *178*, 191.
[38] E. Penzel, N. Goetz, *Die Angewandte Makromolekulare Chemie* **1990**, *178*, 201.
[39] D. Y. Yoon, U. W. Suter, P. R. Sundararajan, P. J. Flory, *Macromolecules* **1975**, *8*, 784.
[40] Z. Xu, N. Hadjichristidis, L. J. Fetters, J. W. Mays, *Adv. Polymer Sci.* **1995**, *120*, 1.
[41] R. B. Karyappa, U. Natarajan, *J. Macromol. Sci., Part B: Physics* **2008**, *47*, 1075.
[42] A. Zioga, N. Ekizoglou, E. Siakali-Kioulafa, N. Hadjichristidis, *J. Polym. Sci. B: Polym. Phys.* **1997**, *35*, 1589.

